# Calculation of the self-formation driving force for composite microstructure in liquid immiscible alloy system*

LIU Xingjun[1,2**], WANG Cuiping[1], Ikuo OHNUMA[2], Ryosuke KAINUMA[2], Kiyohito ISHIDA[2] and CHEN Xiaohu[3]

(1. Department of Materials Science and Engineering, Xiamen University, Xiamen 361005, China; 2. Department of Materials Science, Tohoku University, Sendai 980-8579, Japan; 3. School of Materials Science and Engineering, National Huaqiao University, Quanzhou 362021, China)

Received May 17, 2004; revised October 12, 2004

**Abstract** Using Becker's method, we calculate the interfacial energy between two liquid phases in an immiscible system. Based on the Gibbs-Thomson equation, the force acting on the droplet towards the thermal center can be obtained by integrating the interfacial energy between the droplet and matrix liquid phase, which is related to both the radius of a droplet and the temperature gradient. In addition, the forces of gravitation and buoyancy also act on the droplet. The calculated results indicate that the resultant for these forces together mainly decides the microstructure morphology of the solidified alloy. The calculated results are in good agreement with the corresponding experimental results.

**Keywords:** liquid immiscible alloy system, interfacial energy, composite materials, phase diagram.

In the natural world, there are many immiscible alloy, ceramics and macromolecule systems like oil and water. When these materials are heated to melt on the earth, i.e. under the condition of gravitation, and then directly solidified in a crucible, the materials will form a separated microstructure with the heavier phase at the top, and the lighter one at the bottom, due to the effect of gravitation. Such materials are worthless in practical applications. Much effort has been made to obtain the microstructure with a finely dispersed distribution of both liquid phases[1]. One of the most interesting trials was that in 1979 Ahlborn and Lohberg tried to do an experiment under the micro-gravitation condition for the In-Al alloy to obtain a homogenous two-phase microstructure[2]. However, an unexpected microstructure consisting of two layers with the Al-rich phase at the core of the sample, instead of a uniformly dispersed structure, was obtained, which suggests that it is difficult to obtain a finely dispersed microstructure, even without the influence of gravity. More recently, Wang et al. successfully developed the regular egg-type composite powders and pencil-like bulk composite materials in the immiscible alloy system using atomization and usual solidification processes, respectively[3,4]. Figure 1 shows the egg-type microstructure of the powder and the schematic diagram of the formation process of the microstructure. It is expected that materials with such a microstructure have a wide application because these kinds of composite materials can be obtained in not only alloy system, but also ceramics and macromolecule systems. The formation mechanism was also explained based on the Marangoni equation[5]. The present paper is to give a clearer explanation of the formation mechanism for such composite materials in the liquid immiscible alloy system from the viewpoint of dynamics.

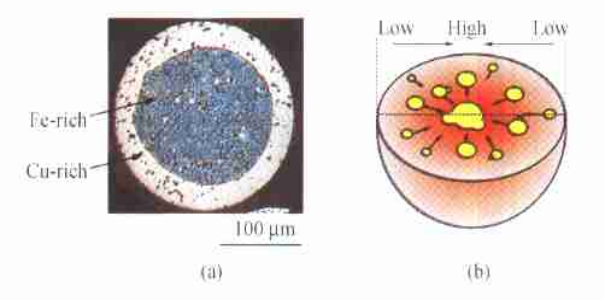


Fig. 1. Microstructure of the Cu-31.4Fe-3Si-0.6C (Weight %) alloy powder; (b) schematic diagram demonstrating the microstructural evolution in the powder.

* Supported by National Natural Science Foundation of China (Grant No. 50271027), Fujian International Cooperation Foundation (Grant No. 2002I018), and Fujian Natural Science Foundation (Grant Nos. E0310023 and 2002J010)

** To whom correspondence should be addressed. E-mail: wangcp@xmu.edu.cn

## 1 Calculation of the interfacial energy between two liquid phases

In a liquid immiscible alloy system, when a liquid phase is cooled into the liquid immiscible region, the second liquid phase (L2) precipitates from the matrix liquid phase (L1). The interfacial energy between the two liquid phases can be calculated based on the Becker's equation[6]

$$\sigma^{L1/L2} \approx \frac{Z^* N^*}{ZN_0} \cdot L_{AB}^{L} (C_B^{L2} - C_B^{L1})^2, \quad (1)$$

where $Z^*$ is the number of cross bonds per front atom, $N^*$ is the number of front atoms per unit area of the interface, $N_0$ is the Avogadro's number, $Z$ is the coordination number, $L_{AB}^{L}$ is the interaction energy between A and B atom, and $(C_B^{L2} - C_B^{L1})$ is the composition difference of the tie-line in the miscibility gap of the liquid phase.

As shown in Fig.2, it is assumed that the liquid droplet (L2) is a sphere, the temperature gradient is $\frac{dT}{dz}$, and the temperature of the center of sphere is $T_0$. Thus, the temperature, interaction energy and composition at any point ($M$) on the surface of the sphere can be expressed by

$$T = T_0 + \Delta T = T_0 + z\frac{dT}{dz}, \quad (2)$$

$$L_{AB}^{L} = A + B \cdot \left(T_0 + z\frac{dT}{dz}\right), \quad (3)$$

$$C_T^{L_1} = C_{T_0}^{L_1} + \Delta C_1, \quad (4)$$

$$C_T^{L_2} = C_{T_0}^{L_2} - \Delta C_2, \quad (5)$$

where $\Delta C_1$ and $\Delta C_2$ are the composition differences of the miscibility gap, which is approximated to be a function of temperature and composition as follows:

$$\Delta C_1 = \alpha_1 \cdot \Delta T = \alpha_1 \cdot z\frac{dT}{dz}, \quad (6)$$

$$\Delta C_2 = \alpha_2 \cdot \Delta T = \alpha_2 \cdot z\frac{dT}{dz}, \quad (7)$$

$$\Delta C_1 + \Delta C_2 = \Delta C = \alpha_1 \cdot z\frac{dT}{dz} + \alpha_2 \cdot z\frac{dT}{dz} = (\alpha_1 + \alpha_2) z\frac{dT}{dz} = \alpha \cdot z\frac{dT}{dz}, \quad (8)$$

$$\alpha_1 = \frac{\Delta C_1}{\Delta T_1}, \quad (9)$$

$$\alpha_2 = \frac{\Delta C_2}{\Delta T}, \quad (10)$$

$$\alpha = \alpha_1 + \alpha_2 = \frac{\Delta C}{\Delta T}, \quad (11)$$

where $\alpha_1$ and $\alpha_2$ are the coefficients associated with the shape of phase diagram, and $\frac{dT}{dz}$ can be determined by the experimental condition; $z$ represents the distance between any point ($M$) and the center ($T_0$) in the $z$ axis direction (Fig.2).

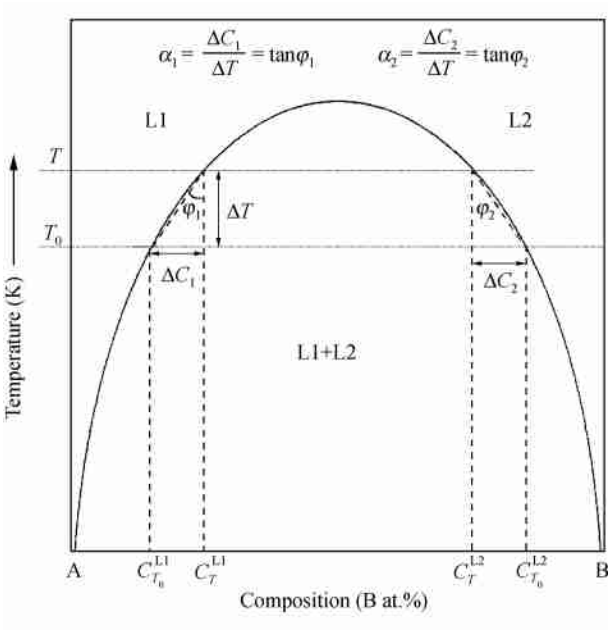


Fig. 2. Phase diagram of A-B binary system with liquid immiscible gap.

Based on Eq. (1), the interfacial energy at any point ($M$) can be expressed by

$$\begin{aligned}
\sigma^{L_1/L_2}(M) &= \frac{Z^* N^*}{ZN_0}\left(A + B\cdot\left(T_0 + z\frac{dT}{dz}\right)\right) \cdot \left(C_{T_0}^{L_2} - \alpha_1 \cdot z\frac{dT}{dz} - C_{T_0}^{L_1} - \alpha_2 \cdot z\frac{dT}{dz}\right)^2 \\
&= \frac{Z^* N^*}{ZN_0}\left(A + B\cdot\left(T_0 + z\frac{dT}{dz}\right)\right) \cdot \left(C_{T_0}^{L_2} - C_{T_0}^{L_1} - \alpha \cdot z\frac{dT}{dz}\right)^2 \\
&= \frac{Z^* N^*}{ZN_0}\left\{ (A + B\cdot T_0)(C_{T_0}^{L_2} - C_{T_0}^{L_1})^2 \right. \\
&\quad + z\left(B \cdot \frac{dT}{dz}(C_{T_0}^{L_2} - C_{T_0}^{L_1})^2 \right. \\
&\quad \left. - 2\alpha \cdot (A + B\cdot T_0)(C_{T_0}^{L_2} - C_{T_0}^{L_1}) \cdot \frac{dT}{dz}\right) \\
&\quad + z^2\left( (-2)\cdot B \cdot \alpha \cdot (C_{T_0}^{L_2} - C_{T_0}^{L_1})\left(\frac{dT}{dz}\right)^2 \right. \\
&\quad \left. + \alpha^2 (A + B\cdot T_0)\left(\frac{dT}{dz}\right)^2\right) \\
&\quad \left. + z^3 \cdot B \cdot \alpha^2 \left(\frac{dT}{dz}\right)^3 \right\} \\
&= \sigma_0 + z\Delta\sigma_1 + z^2\Delta\sigma_2 + z^3\Delta\sigma_3, \quad (12)
\end{aligned}$$

where $\sigma_0$ is the interfacial energy at the temperature of $T_0$, and $\Delta\sigma_1$, $\Delta\sigma_2$ and $\Delta\sigma_3$ are the changes of interfacial energy caused by temperature gradient,

respectively, which are given by

$$\sigma_0 = \frac{Z^* N^*}{ZN_0}(A + B \cdot T_0)(C_{T_0}^{L_2} - C_{T_0}^{L_1})^2, \tag{13}$$

$$\Delta\sigma_1 = \frac{Z^* N^*}{ZN_0}\frac{dT}{dz}(C_{T_0}^{L_2} - C_{T_0}^{L_1})[B \cdot (C_{T_0}^{L_2} - C_{T_0}^{L_1}) - 2 \cdot \alpha \cdot (A + B \cdot T_0)], \tag{14}$$

$$\Delta\sigma_2 = \frac{Z^* N^*}{ZN_0}\left(\frac{dT}{dz}\right)^2[\alpha \cdot (A + B \cdot T_0) - 2 \cdot B \cdot (C_{T_0}^{L_2} - C_{T_0}^{L_1})], \tag{15}$$

$$\Delta\sigma_3 = \frac{Z^* N^*}{ZN_0} B \cdot \alpha^2 \cdot \left(\frac{dT}{dz}\right)^3. \tag{16}$$

From the above equations, it can be seen that when the temperature $T_0$ and the temperature gradient are determined based on the experimental condition, $\sigma_0$, $\Delta\sigma_1$, $\Delta\sigma_2$ and $\Delta\sigma_3$ can be calculated, respectively.

## 2 The force driving a droplet into the thermal center

Based on the Gibbs-Thomson equation, the pressure acting on the droplet with radius $r$ due to the effect of interfacial energy can be expressed by

$$|\boldsymbol{P}(M)| = \frac{2\sigma^{L_1/L_2}(M)}{r}. \tag{17}$$

In Fig. 3, $\boldsymbol{i}$, $\boldsymbol{j}$ and $\boldsymbol{k}$ are the unit vectors in the $x$, $y$ and $z$ directions, respectively. When the surface integral for Eq. (17) is obtained, the force acting on a droplet is

$$F_\sigma = \iint_S \boldsymbol{P}(M) \cdot \boldsymbol{k}\,dA = \iint_S |\boldsymbol{P}(M)| \cos\phi \cdot dA, \tag{18}$$

with $dA = r^2 \sin\phi\, d\phi\, d\theta$.

From Eqs. (17) and (18), we obtain

$$\begin{aligned} F_\sigma &= \int_0^{2\pi}\int_0^{\pi} \frac{2(\sigma_0 + z\Delta\sigma_1 + z^2\Delta\sigma_2 + z^3\Delta\sigma_3)}{r} \cdot \cos\phi r^2 \sin\phi\, d\phi\, d\theta \\ &= 4\pi r\int_0^{\pi}(\sigma_0 + z\Delta\sigma_1 + z^2\Delta\sigma_2 + z^3\Delta\sigma_3) \cdot \cos\phi \sin\phi\, d\phi \\ &= 4\pi r\sigma_0\int_0^{\pi}\cos\phi\sin\phi\, d\phi + 4\pi r^2\Delta\sigma_1\int_0^{\pi}\cos^2\phi\sin\phi\, d\phi \\ &\quad + 4\pi r^3\Delta\sigma_2\int_0^{\pi}\cos^3\phi\sin\phi\, d\phi \\ &\quad + 4\pi r^4\Delta\sigma_3\int_0^{\pi}\cos^4\phi\sin\phi\, d\phi \\ &= \frac{8}{3}\pi r^2\Delta\sigma_1 + \frac{8}{5}\pi r^4\Delta\sigma_3, \end{aligned} \tag{19}$$

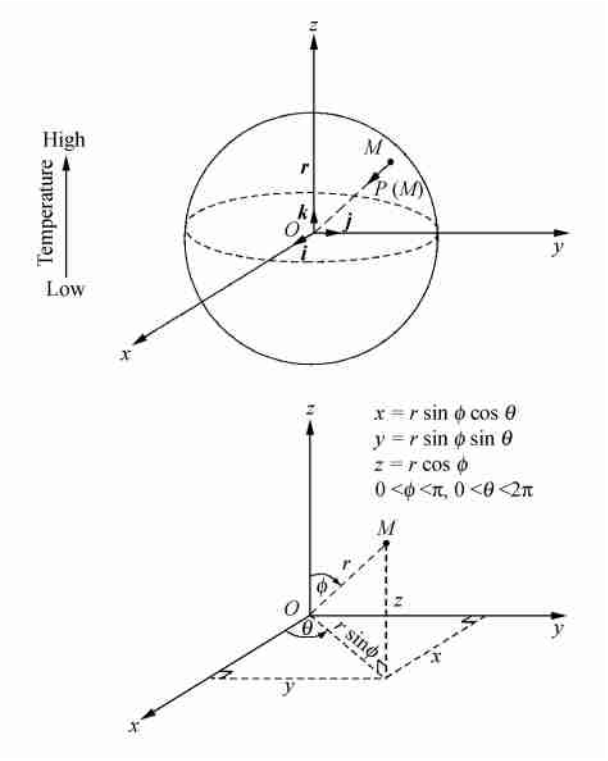


Fig. 3. The spherical coordinates of force analysis on metallic droplet.

where

$$\begin{aligned} \Delta\sigma_1 &= \frac{Z^* N^*}{ZN_0}\frac{dT}{dz}(C_{T_0}^{L_2} - C_{T_0}^{L_1}) \cdot [B \cdot (C_{T_0}^{L_2} - C_{T_0}^{L_1}) - 2\alpha(A + BT_0)] \\ &= \frac{Z^* N^*}{ZN_0}\frac{dT}{dz}(C_{T_0}^{L_2} - C_{T_0}^{L_1}) \cdot \left[B(C_{T_0}^{L_2} - C_{T_0}^{L_1}) - 2\left(\frac{\Delta C}{\Delta T}\right)(A + BT_0)\right], \end{aligned} \tag{20}$$

$$\begin{aligned} \Delta\sigma_3 &= \frac{Z^* N^*}{ZN_0} B\alpha^2\left(\frac{dT}{dz}\right)^3 \\ &= \frac{Z^* N^*}{ZN_0} B\left(\frac{\Delta C}{\Delta T}\right)^2\left(\frac{dT}{dz}\right)^3, \end{aligned} \tag{21}$$

$$\Delta C = (C_T^{L_2} - C_T^{L_1}) - (C_{T_0}^{L_2} - C_{T_0}^{L_1}). \tag{22}$$

As shown in Fig. 2, the value of $\frac{\Delta C}{\Delta T}$ between $T_0$ and $T$ can be obtained from the information of the phase diagram. Thus, the value of $F_\sigma$ can be calculated by Eq. (19). It can be seen from Fig. 4 that the pressure in the cooler side of a droplet is larger than that in the heater side. Thus, the direction of the force ($F_\sigma$) points to the thermal

center.

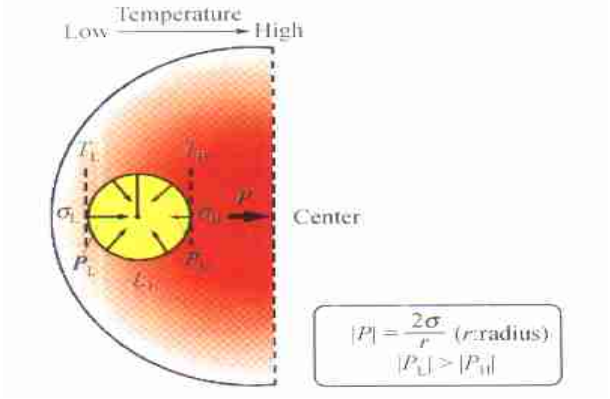


Fig. 4. Schematic digram demonstrating the force evolution in the metallic droplet.

## 3 Application in Fe-Cu base alloy

For simplifying the calculation, as an example, the Fe-Cu binary alloy is discussed in the present work. According to Nishizawa's work[7], $Z^* = 3$, $N^* = 1.7\times10^{19}$ $m^{-2}$ and $Z = 12$. Based on the thermodynamic calculation, the metastable miscibility gap can be calculated, and the value of interaction parameter ($L^{L}_{CuFe}$) can be obtained. Based on Eq. (19), the force driving a droplet to the thermal center can be calculated. As an example, for the Cu-50at. % Fe alloy, when $T_0 = 1550$ K, the calculated result of the force towards thermal center ($F_\sigma$) is shown in Fig. 5. It can be seen that the higher the temperatures, the larger $F_\sigma$ is (i.e. the larger the force acting on a droplet to the center is). On the other hand, when the temperature gradient is a fixed value, the longer the radius of a droplet, the larger $F_\sigma$. This is because there is larger temperature difference between the cooling side (periphery) and the heating side (center) of a droplet.

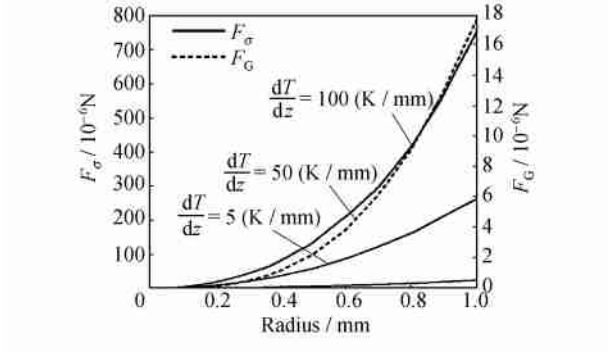


Fig. 5. Calculated $F_\sigma$, $F_G$ versus the droplet radius for different temperature gradients.

Besides the force driving a droplet to the thermal center, the gravitation and buoyancy also simultaneously act on a droplet, which can be expressed by

$$F_G = V\Delta\rho g = \frac{4}{3}\pi r^3\Delta\rho g, \qquad (23)$$

where $\Delta\rho = |\rho^{L1} - \rho^{L2}|$, $\rho^{L1}$ and $\rho^{L2}$ are the densities of L1 and L2 phases, respectively, and g (9.8 m/s$^2$) is the gravity coefficient. Figure 5 shows the relationship between $F_G$ and the radius of a droplet. It can be seen that the larger the radius is, the larger $F_G$ is, due to the effect of gravitation.

From Eqs. (19) and (23), the following equation can be obtained:

$$F_{\sigma/G} = \frac{F_\sigma}{F_G} = \frac{A}{r} + Br,$$
$$(0 \leqslant r \leqslant (T - T_0)/(dT/dz)), \qquad (24)$$

where $A = \frac{2\Delta\sigma_1}{\Delta\rho g}$, $B = \frac{6\Delta\sigma_3}{5\Delta\rho g}$.

In fact, $F_\sigma$ and $F_G$ determine the motion direction of a droplet on cooling, which basically decides the microstructure morphology of an alloy, although the viscosity of the liquid phase also has effect on the microstructure morphology. Figure 6 shows the relationship between $F_{\sigma/G}$ and the temperature gradient as well as the radius of a droplet. It is seen that the value of $F_{\sigma/G}$ is larger when the radius is smaller, which means that $F_\sigma$ is dominant and the value of $F_{\sigma/G}$ rapidly decreases when the radius is larger than a certain value.

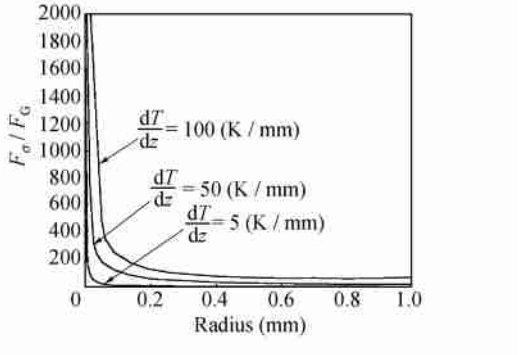


Fig. 6. The calculated $F_\sigma/F_G$ ratio versus the droplet radius for different temperature gradients.

By combining the present calculated results with our previous experimental results[3,4], the relationship between the temperature gradient and the microstructure morphology can be summarized as follows: (1) when the temperature gradient is very

large, the force acting on a droplet ($F_\sigma$) is a decisive factor, and the effect of gravitation can be omitted. For example, for the powder made by atomization process, the egg-type composite powder can be formed, because there is a very large temperature gradient from the surface to the thermal center of a powder[3]; (2) when the temperature gradient is larger, besides the force acting on the droplet moving to the center, $F_\sigma$ also has the effect on the movement of a droplet. For example, under the condition of conventional solidification, the pencil-like bulk composite materials with different sizes of core and periphery can be obtained due to the effect of gravitation[4]; (3) when the temperature gradient is very small (for example, the molten alloy is directly cooled in a crucible), $F_G$ is dominant because $F_\sigma$ tends to zero. The growth of the droplets result in that the effect of gravitation is larger and larger. Finally, the bulk alloys with the microstructure of the top and bottom layers are formed due to the effect of gravitation.

## 4 Conclusions

By calculating the interfacial energy between the two liquid phases, it is found that the interfacial energy depends on the temperature gradient. The direction of the force acting on a droplet is to the high temperature region of a droplet, i.e. the center of a droplet. This is the reason why the composite microstructure with the core and periphery during cooling is formed. The present results are in agreement with those obtained by Marangoni equation previously[3], and can more clearly explain the mechanism of composite microstructure formation.

## References


1 Predel B. Constitution and thermodynamics of monotectic alloys—a survey, In: Thermodynamics of Alloy Formation, (eds. Chang Y. A. and Sommer F.), Warrendale, PA, The Minerals, Metals and Materials Society, 1997, 1—19.

2 Ahlborn H. and Lohberg K. Aluminium-indium experiment SOLUOG—a sounding rocket experiment on immiscible alloys. In: 17th Aerospace Science Meetings, American Institute of Aeronautics and Astronautics, New York, 1979, 3—7.

3 Wang C. P., Liu X. J., Ohnuma I. et al. Formaiton of immiscible alloy powders with egg-type microstructure. Science, 2002, 297: 990—993.

4 Wang C. P., Liu X. J., Takaku Y. et al. Formation of core-type macroscopic morphologies in Cu-Fe base alloys with liquid miscibility gap. Metall. Mater. Trans. A, 2004, 35A: 1243—1253.

5 Marangoni C. Ueber die ausbreitung der tropfen einer flüssigkeit auf der oberfläche einer anderen. Ann. Phys. Chemie (in German), 1871, 143: 337—340.

6 Becker R. Die keimbildung bei der ausscheidung in metallischen mischkristallen. Ann. Physik (in German), 1938, 32: 128—133.

7 Nishizawa T., Ohnuma I. and Ishida K. Correlation between interfacial energy and phase diagram in ceramic-metal system. J. Phase Equilibria., 2001, 22: 269—278.

8 Chen Q. and Jin Z. P. The Fe-Cu system: a thermodynamic evaluation. Metall. Mater. Trans. A, 1995, 26A: 417—428.